Mid-IR Spectroscopy of the Diffuse Ionized Halo of NGC 891

Richard J. Rand[1], Kenneth Wood[2], Robert A. Benjamin[2],

ABSTRACT

The sources of ionization and heating of the diffuse ionized gas in spiral galaxy disks and halos remain unclear. The usual optical diagnostic line ratios suffer from dependence on a confusing number of variables: not only the ionization state but also the temperature and abundance of the gas, as well as extinction. The Spitzer Space Telescope provides the opportunity to study the [Ne III]/[Ne II] mid-IR diagnostic, for which temperature, gas-phase abundance and extinction (although see below) effects are unimportant. Here we report the first detection of these lines in a spiral galaxy halo, and find that the ratio is enhanced in the halo relative to the disk. Using a 2-D Monte Carlo-based photo-ionization code which accounts for the effects of radiation field hardening, we find that this trend cannot be reproduced by any plausible photo-ionization model. We also report the first spectroscopic detections of PAH molecules in an external galaxy halo. Their emission suggests rough scale-heights of 300–500 pc.

Subject headings: galaxies: ISM — galaxies: spiral — galaxies: individual(NGC 891 — methods: numerical

1. Introduction and Observations

The Diffuse Ionized Gas (DIG, or in the Milky Way, the Reynolds Layer) accounts for the vast majority of free electrons in typical spirals. Yet a complete understanding of the sources of ionization and heating of this gas remains unclear. Energetically, photo-ionization by massive stars must dominate, but ionizing photons must travel 100's–1000's of pc from their ionizing sources. Optical emission line ratios such as [N II]/Hα, [S II]/Hα, [O III]/Hβ, and [O I]/Hα and their spatial variations confirm the viability of photo-ionization, but models have difficulty explaining the observed trends. In particular, in several galaxy halos such

[1]University of New Mexico

[2]University of St. Andrews

[2]University of Wisconsin-Whitewater

as that of NGC 891, all of these ratios rise with distance, z, from the thin disk of massive stars (e.g. Figure 3), whereas basic models (e.g. Domgörgen & Mathis 1994) predict that [N II]/Hα and [S II]/Hα should rise while [O III]/Hβ should fall as the gas moves to a lower ionization state due to the increasing dilution of the radiation field.

The rise of [O III]/Hβ with z in NGC 891 and NGC 5775 has been modeled by Rand (1998) and Collins & Rand (2001) as reflecting a combination of photo-ionization and a growing contribution (with z) from shock ionization in the halo. Alternatively, the fact that all of these gas-temperature-sensitive ratios are frequently seen to rise with distance from HII regions has led to the suggestion that it is temperature, rather than ionization state, which changes with distance from ionizing sources (Reynolds, Haffner, & Tufte 2003). However, Collins & Rand (2001) find that this effect is insufficient to explain the high [O III]/Hβ values in the halos of NGC 5775 and UGC 10288. Models incorporating hardening of photo-ionizing radiation fields due to initial propagation through HII regions ("leaky HII region" models) help increase line ratios (e.g. Hoopes & Walterbos 2003; Wood & Mathis 2004) but still have difficulty explaining all ratios simultaneously.

A significant problem is that the ratios are sensitive not only to the ionization state, but also to the gas-phase temperature and abundances, as well as extinction, which has been shown to be significant up to z=2 kpc in some edge-ons, including NGC 891 (Howk & Savage 1999, 2000). The He Iλ5876/Hα ratio provides tighter constraints on the ionization state, but the He line is very faint and data are scarce (Rand 1997; Hoopes & Walterbos 2003). The Spitzer Space Telescope allows access to the [Ne II] 12.8μm and [Ne III] 15.6μm lines. Their ratio forms an ionization diagnostic relatively insensitive to temperature, abundance and extinction. The first two IPs of Ne are 21.6 and 41.0 eV, thus probing the harder end of the UV spectrum. Here we report the first detections of these lines in a galaxy halo, that of NGC 891, using the IRS (Houck et al. 2004) SH module, providing coverage from 9.9 to 19.6 μm at $R \approx 600$. We observe a disk field (0.5 hours) and two halo fields (6.7 hours each) at $z \approx 1$ kpc (Figure 1). The data were taken in Cycle 2 (program ID: 20380). [S III] 18.71 μm and the 17.03 μm H_2 rotational line are also detected in the disk and halo. We detect spectroscopically several PAH features in an external galaxy halo for the first time. Spectra are shown in Figure 2. We also reduced some disk pointings from GTO time for comparison.

2. Results

Figure 3 shows that the [Ne III]/[Ne II] ratio is higher in the halo than in the disk – a strong indication that the ionization state in the halo for species with IPs in the 20-40 eV range is indeed higher than in the disk, and that a temperature increase alone cannot explain

the behavior of the optical line ratios. The disk ratios in the GTO data are all consistent with our value. Figure 3 also shows optical emission line ratios from Rand (1998) along the long-slit indicated in Figure 1.

As an aside, we note that extinction near the midplane may be significant even at mid-IR wavelengths, although the extinction law in this part of the spectrum is very uncertain. From CO and HI maps in the literature, assuming standard Galactic gas and dust relations, and a value of $A_{15\mu m}/A_K$ of 0.4, consistent with determinations for many directions in the Galactic plane by Jiang et al. (2006), we estimate that there could be about 2 magnitudes of extinction at 15 μm at our disk position. Extinction at $z = 1$ kpc is negligible. The possible effect of reddening on [Ne III]/[Ne II] is even less well constrained. If we use the extinction at 12 μm towards the Galactic Center from Lutz (1999), which exceeds that at 15 μm, the disk neon ratio would be further lowered relative to the halo ratios.

Figure 4 illustrates results from a typical 2-D Monte Carlo photo-ionization model (see Wood & Mathis 2004). These models incorporate hardening of the radiation field as it propagates, which may be important for explaining the behavior of some of the optical line ratios in the Reynolds Layer (Wood & Mathis 2004). The gas density distribution is chosen to match that in NGC 891. We have explored a range of temperatures (from 40kK to 50kK) and luminosities for the ionizing spectrum, and considered "leaky" models in which the input spectrum is that from a spherical 40kK simulation which has its physical size set to allow 15% of the ionizing photons to escape. This leaky model suppresses the He-ionizing photons with energies above 24.6 eV and hardens the spectrum in the H-ionizing continuum. Generally, while such models can semi-quantitatively reproduce the behavior of [N II]/Hα and [S II]/Hα (not shown), they overpredict [Ne III]/[Ne II], and predict that the ratio should fall with z, as Figure 4 shows. The models also predict a falling [O III]/Hα with z (Figure 4), contrary to the observation. Also not shown, the modeled [O I]/Hα values are generally too low, and He I/Hα is not well matched. These results demonstrate that hardening of the radiation field is insufficient to explain the data. An extra source of non-ionizing heating will not affect the neon ratio as the ratio is insensitive to gas temperature. The neon results therefore indicate that additional sources of ionization of DIG must be considered.

Table 1 shows not only the intensities of the gas-phase lines discussed above but also the intensities and equivalent widths (EWs) of PAH features at 11.2, 12.0, 12.7, 16.5, and 17.4 μm. A broad plateau from 16.5 to 17.5 μm is also detected (Figure 2). PAHs emitting in the 10–20 μm range are thought to be generally neutral and larger than PAHs emitting shortward of 10 μm (Draine & Li 2007). The main results for the PAH features are as follows. If the emission depends exponentially on z, the emission scale-heights are roughly $300 - 500$ pc. For two magnitudes of extinction in the disk, this range would become $210 - 270$ pc.

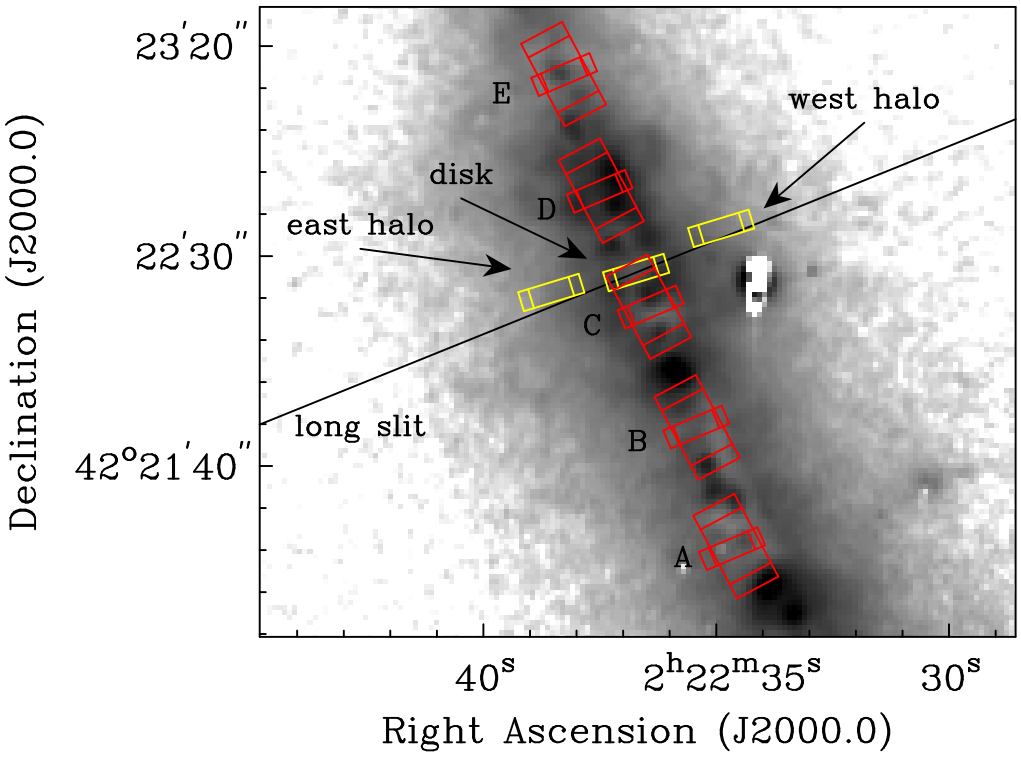

Fig. 1.— Section of an Hα image of NGC 891 (Rand, Kulkarni, & Hester 1990). Boxes show IRS pointings (for each pointing, two overlapping boxes, showing the two nods, are drawn). The three (yellow) boxes are the IRS SH pointings discussed here. The other (red) boxes in the disk show pointings for the SH and LH GTO data mentioned. The solid line shows the orientation of the slit for the optical emission line data discussed. The slit width is 2.25″. The white blotch in the Hα image is an artifact of continuum subtraction of a foreground star.

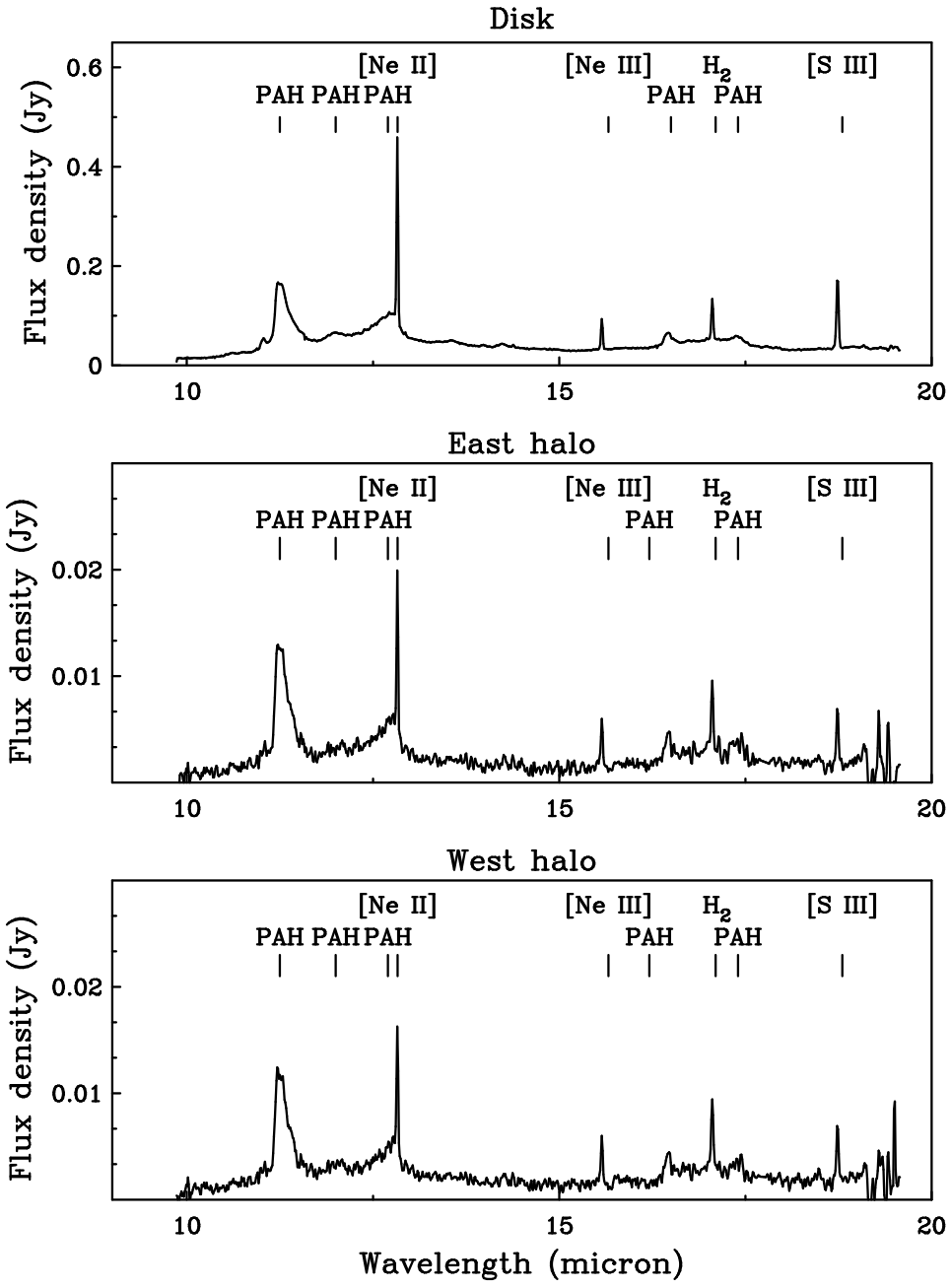

Fig. 2.— IRS SH spectra of the disk, East halo and West halo fields of NGC 891. Detected gas and dust phase features are indicated.

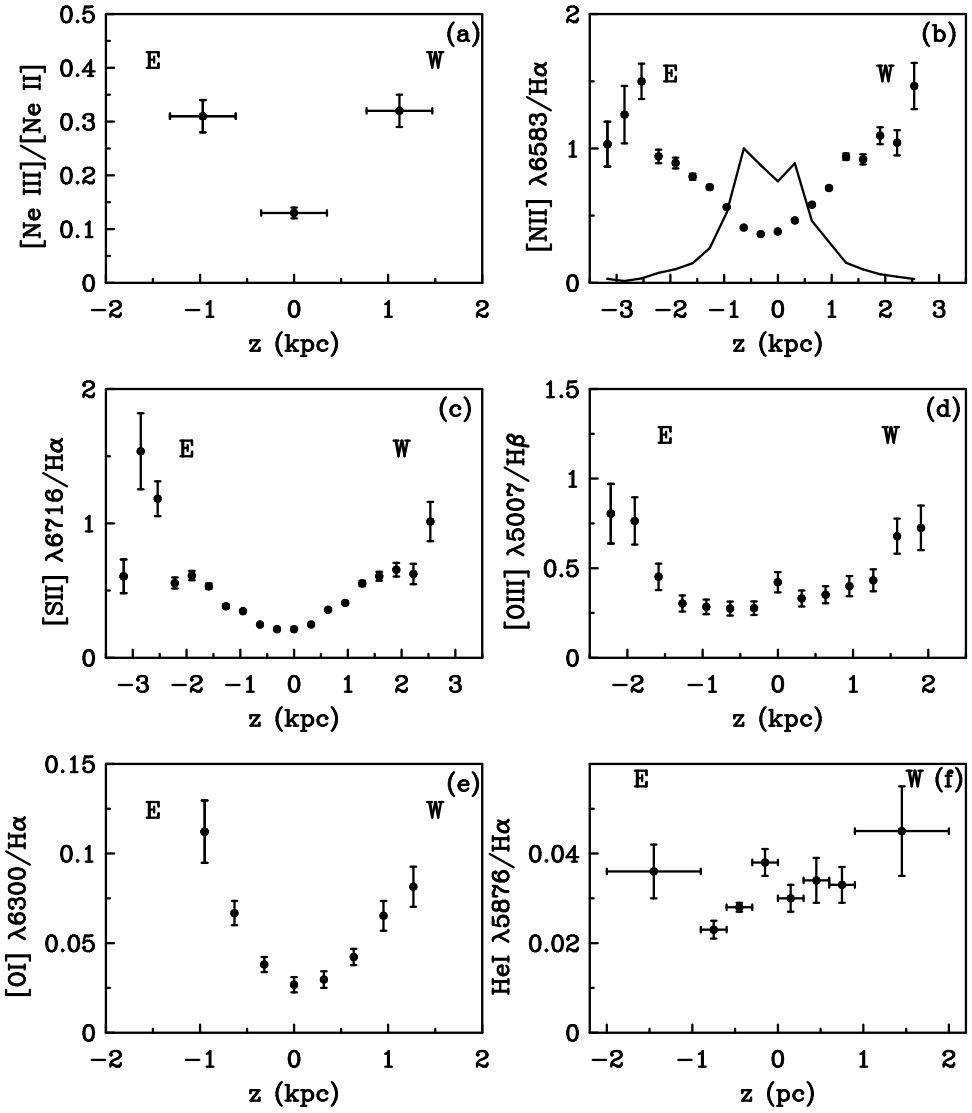

Fig. 3.— Dependence of (a) [Ne III]/[Ne II], (b) [N II]λ6583/Hα, (c) [S II]λ6716/Hα, (d) [O I]λ6300/Hα (e) [O III]λ5007/Hβ, and (f) He I λ5876/Hα on z. The optical line ratios are from Rand (1997, 1998). The Hα profile, normalized to unit intensity, from Rand (1998), is shown in (b). Horizontal error bars in (a) and (f) reflect the extent over which the data have been averaged. In the other panels, the intensities were averaged over 317 pc.

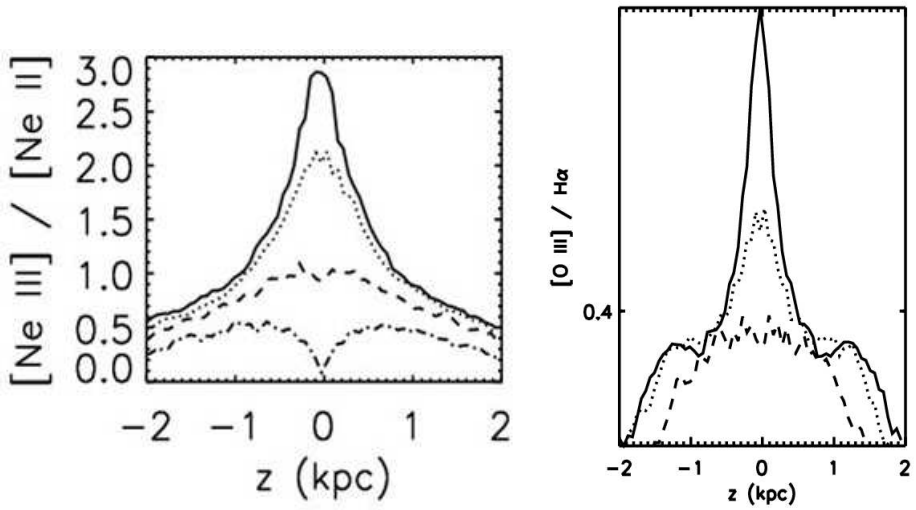

Fig. 4.— [Ne III]/[Ne II] and [O III]/Hα vs. z for for a typical 2-D photo-ionization model. The solid, dotted, dashed and dot-dashed lines are for lines of sight through an ionization cone at 0, 0.3, 0.6, and 0.9 kpc from the center. The effective temperature of the ionizing radiation field is 40kK.

Table 1. Infrared Line Intensities and PAH Equivalent Widths

Line	Disk Intensity[a]	Disk EW (μm)	Halo East Intensity	Halo East EW (μm)	Halo West Intensity	Halo West EW (μm)
[S IV] 10.51 μm	<1.9[b]		<1.0		<1.1	
[Ne II] 12.81 μm	320 ± 20		12 ± 1		11 ± 1	
[Ne III] 15.56 μm	41 ± 3		3.8 ± 0.4		3.4 ± 0.3	
[S III] 18.71 μm	87 ± 6		3.0 ± 0.3		3.0 ± 0.3	
H_2 $S(1)$ $J = 3 - 1$ 17.03 μm	49 ± 3		4.0 ± 0.3		4.3 ± 0.3	
PAH[c] 11.2 μm	1400 ± 100	0.85 ± 0.04	105 ± 9	0.99 ± 0.05	89 ± 7	0.77 ± 0.04
PAH 12.0 μm	85 ± 7	0.043 ± 0.002	2.5 ± 0.9	0.02 ± 0.01	4.7 ± 0.8	0.04 ± 0.01
PAH 12.7 μm	600 ± 50	0.32 ± 0.02	36 ± 3	0.36 ± 0.02	23 ± 2	0.21 ± 0.01
PAH 16.5 μm	68 ± 5	0.08 ± 0.01	4.0 ± 0.5	0.08 ± 0.01	3.6 ± 0.4	0.08 ± 0.01
PAH 17.4 μm	32 ± 2	0.038 ± 0.002	5.5 ± 0.6	0.12 ± 0.01	3.6 ± 0.4	0.08 ± 0.01

[a]Units are (10^{-17} erg cm^{-2} s^{-1} arcsec^{-2})

[b]Upper limits are 3σ.

[c]Intensities for the 11.2 μm feature include the secondary peak at about 11.0 μm.

For the 11.2 and 12.7 μm features (the only ones detected in all five GTO pointings), the scale-heights change insignificantly if we use instead the average of the disk intensities in the GTO observations. Only the 17.4 μm feature stands out as having a higher disk-halo contrast than the others, in both intensity and EW. This feature's origin is uncertain, but is thought to arise from large, neutral PAHs (Peeters et al. 2004). Hence there is slight evidence that the halo favors larger PAHs relative to the disk.

We thank G. Stacey for a brief but useful discussion about extinction in the mid-IR. This work is based (in part) on observations made with the *Spitzer Space Telescope*, which is operated by the Jet Propulsion Laboratory, California Institute of Technology under a contract with NASA. Support for this work was provided by NASA through an award issued by JPL/Caltech.

REFERENCES

Collins, J. A., & Rand, R. J. 2001, ApJ, 551, 57

Domgörgen, H., & Mathis, J. S. 1994, ApJ, 428, 647

Draine, B. T., & Li, A. 2007, ApJ, 657, 810

Hoopes, C. G., & Walterbos, R. A. M. 2003, ApJ, 586, 902

Houck, J. R., et al. 2004, ApJS, 154, 18

Howk, J. C., & Savage, B. D. 1999, AJ, 117, 2077

Howk, J. C., & Savage, B. D. 2000, AJ, 119, 644

Jiang, B. W., Gao, J., Omont, A., Schuller, F., & Simon, G. 2006, A&A, 446, 551

Lutz, D. 1999, in ESA Special Publication, Vol. 427, The Universe as Seen by ISO, ed. P.Cox & M.Kessler, p. 623

Peeters, E., Spoon, H. W. W., & Tielens, A. G. G. M. 2004, ApJ, 613, 986

Rand, R. J. 1997, ApJ, 474, 129

Rand, R. J. 1998, ApJ, 501, 137

Rand, R.J., Kulkarni, S. R., & Hester, J. J. 1990, ApJ, 352, L1

Reynolds, R. J., Haffner, L. M., & Tufte, S. L. 2003, ApJ, 525, 21

Wood, K., & Mathis, J. S. 2004, MNRAS, 353, 1126